Design of Peptide Hybrid Nanostructured Magnetic Materials for Biomedical Applications

A thesis submitted towards the partial fulfilment of

BS-MS dual degree programme

By

ANAGHA M. C.

(BS-MS student, Registration No.: 20121007)

Under the guidance of

Dr. Seema Verma

Department of Chemistry
Indian Institute of Science Education and Research (IISER) Pune, India

CERTIFICATE

This is to certify that this dissertation entitled "**Design of Peptide Hybrid Nanostructured Magnetic Materials for Biomedical Applications**" towards the partial fulfilment of BS-MS dual degree programme at the Indian Institute of Science Education and Research, Pune represents original research carried out by **Anagha M C** at IISER Pune under the supervision of "**Dr. Seema Verma**, Faculty Fellow, Department of Chemistry, IISER Pune" during the academic year of 2016-2017.

Seema Verma

Date: 20/3/2017

Place: Pune

Dr. Seema Verma

Faculty Fellow
Department of Chemistry
IISER Pune

DECLARATION

I hereby declare that the matter embodied in the report entitled "**Design of Peptide Hybrid Nanostructured Magnetic Materials for Biomedical Applications**" are the results of the investigations carried out by me at the Department of Chemistry, IISER Pune, under the supervision of **Dr. Seema Verma** and the same has not been submitted elsewhere for any other degree.

Anagha M C

Date: 20/03/2017

Place: Pune

ACKNOWLEDGEMENTS

I would like to express my sincere gratitude to **Dr. Seema Verma** for her continuous support, guidance, scientific advices and encouragement throughout the project. I would take this opportunity to sincerely thank **Dr. H. N. Gopi** for the continuous support and guidance in peptide synthesis and providing me an opportunity to work in his lab.

I would also like to thank **Dr. Sunil Nair** for providing the magnetic data.

My sincere thanks go to Ms. Anindita Adak for helping me in the peptide synthesis and training me in the initial days of peptide work.

I'm extremely thankful to my lab mates and friends Surya, Nithinraj and Sereena for their kind help and co-operation during the project days. I would like to thank other lab members also for being friendly and supportive.

I'm thankful to Mr. Mahesh for all TGA measurements. I would like to thank FESEM, NMR and MALDI/TOF operators also for all the instrumentation help.

Last but not the least I would take this opportunity to thank my family and friends for their support and love.

TABLE OF CONTENTS

List of illustrations

List of abbreviations

CPP – Cell Penetrating Peptide

CTAB – Cetyl trimethyl ammonium bromide

DCC – N, N'- Dicyclohexylcarbodiimide

DCM – Dichloromethane

DMAP – 4-Dimethylaminopyridine

DMF – Dimethylformamide

FC – Field-cooled

FITC – Fluorescein isothiocyanate

FTIR – Fourier Transform Infrared Spectroscopy

HBTU – O-Benzotriazole-N,N,N',N'-tetramethyluronium hexafluorophosphate

HOBt – 1-Hydroxybenzotriazole

HPLC – High Performance Liquid Chromatography

MNP – Magnetic nanoparticles

NMP – N-Methyl-2-pyrrolidone

PXRD – Powder X-ray Diffraction

TAT – Trans-activating transcriptional activator

TEOS – Tetraethyl orthosilicate

TFA – Trifluoroacetic acid

TGA – Thermogravimetric analysis

ZFC – Zero-Field cooled

ABSTRACT

Cell penetrating peptides have attracted much attention as a potential chemotherapeutics in recent years. However, there is a clear need to develop strategies to overcome the lack of target specificity. Magnetic nanoparticles (MNP), on the other hand represent a promising agents for specifically treating cancer cell by drug delivery and magnetic fluid hyperthermia. Also, magnetic nanoparticles functionalized with fluorescent dyes have been utilized for optical imaging as bio - labeling agents. In the present work, we aim to integrate the cell penetrating peptides attached to a fluorescent marker with magnetic nanoparticles. This allows us to get water dispersible peptide hybrid multifunctional magnetic nanostructures, suitable for biomedical applications particularly to specifically treat the cancerous cells. In this end, peptides of different functionality were systematically synthesized by solution and solid phase synthetic methods. The purity of different peptides was further characterized by MALDI / TOF and NMR spectra. The present study demonstrates a method to achieve water dispersible $CoFe_2O_4$ and γ-Fe_2O_3 nanoparticles by a thermal decomposition method using N-methyl 2-pyrrolidone (NMP) as solvent and peptides as a capping agent and a stabilizer. This will allow us to extend the same protocol to integrate iron oxide and cobalt ferrite nanoparticles with a fluorescent dye attached cell penetrating peptides, ideal for biomedical applications. The phase purity of the peptide hybrid nanostructured materials were examined by powder X-ray diffraction (XRD) patterns. The structural and thermal behavior of the nanoparticles was further characterized by Fourier transform infrared spectroscopy (FTIR) and thermogravimetric analysis (TGA) respectively. The magnetization studies were carried out using a Quantum Design MPMS SQUID magnetometer. The presence of fluorescent dye was confirmed by UV-VIS and Photoluminescence (PL) spectroscopy.

CHAPTER I

INTRODUCTION

This chapter at the beginning demonstrates a brief introduction on magnetic nanoparticles and their extended applications on integrating it with peptides. We have also presented a brief review of literature on magnetic nanoparticles and peptides separately.

1.1 INTRODUCTION

With the advent of nanotechnology the research on magnetic nanomaterials has intensified during the past few decades. Biomedicine, targeted drug delivery, magnetic hyperthermia, MRI imaging have become key areas of research harnessing the various unique properties of magnetic nanomaterials.[1,2] Though, there are many reports on the synthesis of high quality magnetic nanoparticles in non-polar solvent, stabilization of nanoparticles by non-degradable surfactant hampers its application in bio-related fields. Therefore, focus has been given on the synthesis of water dispersible magnetic nanoparticles with controllable size and desirable surface functionalities and indeed this continue to remain a significant challenge in the area of nanoparticle synthesis of good quality. Peptides on the other hand, are known for their structural diversity due to their ability to arrange the amino acids in secondary structural elements which in turn can act as a good template, reducing and capping agents for the synthesis of multifunctional hybrid materials of ordered shape and size.[3,4] Also, it is well documented that some of the bioactive peptides play an important role in a broad range of physiochemical conditions. However, the limitations of peptides include (i) poor stability and solubility in water under physiological conditions due to its amphipathic structure and (ii) lack of targeting ability towards cancer cells. This can be largely addressed by functionalizing peptides with the magnetic nanoparticles which can be remotely controlled by applying the external magnetic field thereby affording cancer cell-targeting capabilities. Furthermore, peptides with appropriate biocompatible surface functionalities appropriately attached to fluorescein isothyocyanate (FITC) may not only act as an effective capping agent and stabilizer for functionalizing the magnetic nanoparticles but it can also be used as an effective biomarker. In the present work, we aim to conjugate the cell penetrating fluorescent peptides with the magnetic nanoparticles. The synergistic effect of magnetic nanoparticles and fluorescent cell-penetrating peptides will not only help us to enhance cellular uptake, it can also allow the hybrid nanostructures as a good magnetic resonance imaging contrast agent (MRICA) which can afford localized heating (hyperthermia) in presence of ac field.

1.2 Magnetic nanoparticles

With the advent of nanotechnology the research on magnetic nanomaterials has intensified during the past few decades. It has shown a great potential for technological applications like information storage and electronic devices. Magnetic nanoparticles have promising potential in biomedical applications also because of the unique abilities of magnetic interaction. They have been extensively used for their application like magnetic resonance imaging,[5,6] biotechnology, tissue engineering, bio sensing[7] and targeted drug delivery.[8,9] Magnetism in the matter originates from the spin and orbital magnetic moments associated with the electrons. Based upon the interaction of magnetic moments vectors and their magnitude, variety of magnetic ordering is known which are classified as paramagnetic, ferromagnetic, ferrimagnetic and antiferromagnetic. In paramagnetic materials, all magnetic moments are randomly oriented and cancel out each other. In order to attain a saturated magnetization where all magnetic moments are aligned in the same direction of applied field, a high magnetic field is required with very low temperature. Ferro- and ferrimagnetic materials in the absence of field are divided into small regions called domains. Individual domains are spontaneously magnetized and the directions of magnetization of domains are random and cancel out each other. The process of magnetization involves the change of multidomain material into single domain. The dependence of magnetization with applied field is not linear in the case of ferro- and ferrimagnetic materials and is shown in Figure 1.1. As the strength of field increases magnetization also increases and reaches to its maximum value called saturation magnetization, M_s. Once the magnetization is saturated; decrease in field to zero doesn't decrease magnetization to zero. There will be a remnant or residual magnetization M_R present in the material. In order to make the magnetization zero, a field has to be applied in the opposite direction which is called coercive field H_C. The characteristic field dependent (M-H) curve gives magnetic hysteresis loop. The process of magnetization is governed by (i) domain wall motion at low field and (ii) domain rotation at high field.

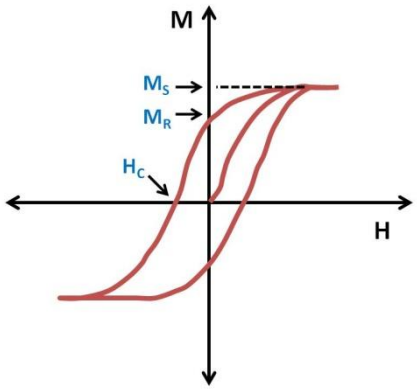

Figure 1.1: Field dependent (M-H) magnetization

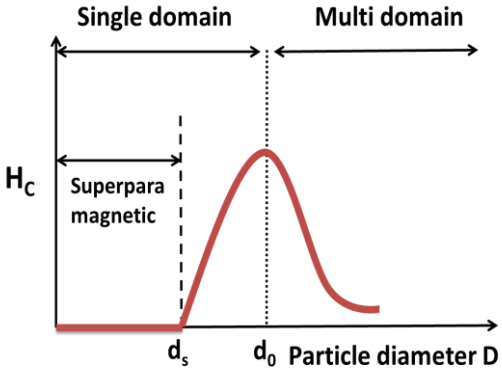

Figure 1.2: Particle size dependence of coercivity

As the size reduces, the formation of domain walls becomes energetically unfavorable so the multi domain particles become single domain. As single domain particles have uniform magnetization with minimum free energy, magnetization reversal requires strong field in order to coherently rotate the magnetic moment vectors, thereby enhancing the coercivity for such particles. Therefore, coercivity has a striking dependence upon the size of the particles and such dependence is represented in the Figure 1.2. It is clear that as the size decreases the coercivity increase and has a maximum value for single domain particles (d_0). Further decrease in the size decreases the coercivity and becomes zero below a critical size (d_s). In order to understand this, consider an assembly of single-domain particles, each with anisotropy energy density $E= K \sin^2\theta$. Here θ is the angle between Ms and the easy axis and K is the anisotropy constant. The magnetization can be reversed by changing the direction of magnetization from one easy axis of magnetization (preferred crystallographic axis) to the other. In order to do this, it should overcome an energy barrier ΔE which is equal to KV where V is the volume of particles. Ne´el pointed out that when size of the particles decreases and become small enough then ΔE become so small so that thermal fluctuations can overcome the energy barrier and reverse the magnetization even in the absence of an applied field. When E_A and thermal activation energy k_BT (k_B is the Boltzman constant) becomes comparable, the direction of magnetization starts flipping and causes faster relaxation from one easy axis to another. Therefore, even if the particles are associated with huge magnetic moment it behaves like paramagnets. Such type of behavior is called

superparamagnetism. For example, in typical paramagnetic materials the magnetic moment per atom is only a few Bohr magnetons. However, a spherical particle of iron 50Å in diameter contains 5560 atoms and has the relatively enormous moment of (5560) (2.2) = 12,000 μ_B. These particles show paramagnetic behavior as well as gives high magnetic moment and hence they are called superparamagnetic materials.[10] In order to study such superparamagnetic particles we need to cool down the samples as below a typical temperature called blocking temperature, T_B, the thermal energy becomes lower than the anisotropy energy and the superparamagnetic particles starts relaxing slower. Superparamagnetic particles are characterized by zero-field-cooled (ZFC) and field-cooled (FC) susceptibility. The temperature corresponding to the maximum magnetization in ZFC is the superparamagnetic blocking temperature T_B below which both ZFC and FC magnetization bifurcates. Such temperature dependent magnetization curves of FC and ZFC are the characteristic features of superparamagnetism. Typical low temperature magnetization behavior and the expected opening of the hysteresis loop are shown in the Figure 1.3. Therefore, superparamagnetism is a unique properties associated with the tiny magnetic nanoparticles which can also be controlled by adjusting the anisotropy energy barrier, E_A.

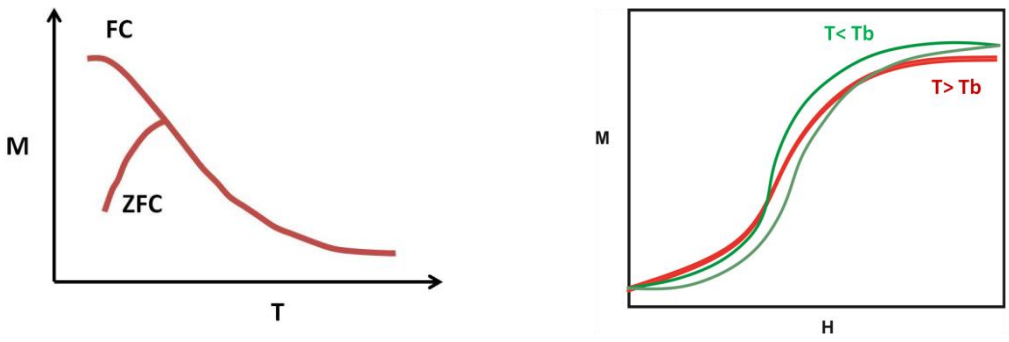

Figure 1.3: Temperature dependent ZFC and FC magnetization curves (left) and field dependent magnetization curves below and above blocking temperature of superparamagnetic nanoparticles (right).

1.3 Peptides

Proteins are the most abundant organic molecules present in organisms and plays important roles in cell structure and functions. Nature has used millennia of evolution to design and modify peptides with different functionalities like hormones, [11] antibodies for molecular recognition, [12] enzymes for catalysis, oligonucleotides and so on.

The building blocks of peptides and proteins are amino acids with general formula H_2N-CHR-COOH shown in Figure 1.4. Based on the R group, amino acids are classified as non-polar, polar, acidic, and basic. The presence of carboxylic group and amine group makes them behave as both acidic and basic. Most abundant amino acids are protein constituents and are always α-amino acids. Glycine, glutamate, γ-amino butyric acid (derivative of glutamate) acts as neurotransmitter. Thyroxine and indole acetic acid (derivatives of tyrosine and tryptophan) are hormones. Amino acids that are not constituent of proteins also occur in living organisms which play important roles in cellular metabolism. Homocysteine and homoserine are amino acids that are not constituents of proteins and act as a precursor in the biosynthesis of methionine.

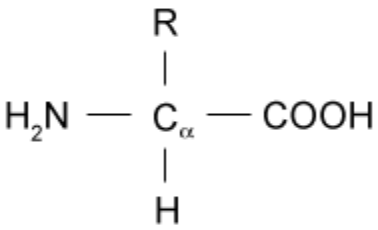

Figure1.4: General structure of amino acid

Amino acids are connected through peptide bond between carboxylic end of one amino acid and amine end of other amino acid which makes them strong. The amino acid residue with free amine is called N-terminus and is written to the left. Similarly the residue with free carboxylic acid is called C-terminus and is written to the right. Figure 1.5 shows the schematic diagram of peptide bond formation.

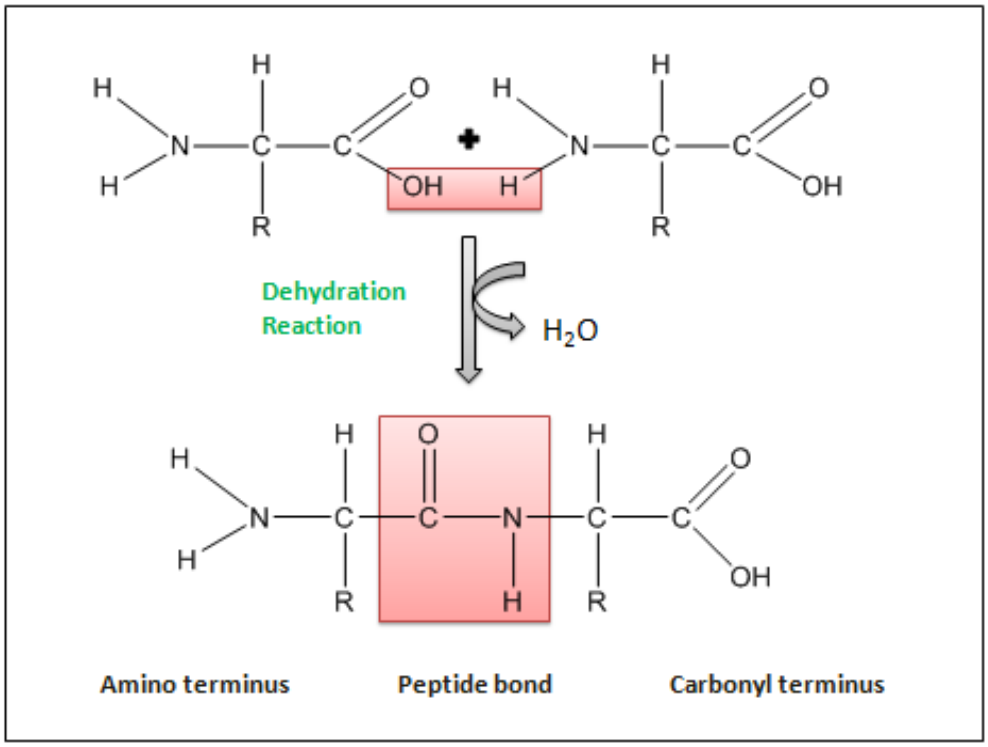

Figure1.5: Schematic picture of peptide bond formation

The structure of peptides and proteins are described as having four levels which is shown in Figure 1.6. First one is the primary structure which is nothing but the sequential arrangements of amino acids one after the other. The secondary constitute the second level of protein structure. It arises due to the regular folding of polypeptide chains due to the intermolecular hydrogen bonding between the electro negative carbonyl oxygen atom of one amino acid and the amide hydrogen atom of another amino acid. It can be coiled to form α-helix structure or can be stretched out to form β-pleated structure.[13] Tertiary structure results from the bending and folding of peptide chains. Ionic bonding, hydrogen bonding, disulfide linkage, dispersion forces are the major interactions which determines the shape, size and stability of the tertiary proteins. Arrangements of different tertiary structures results in the formation of quaternary structures.

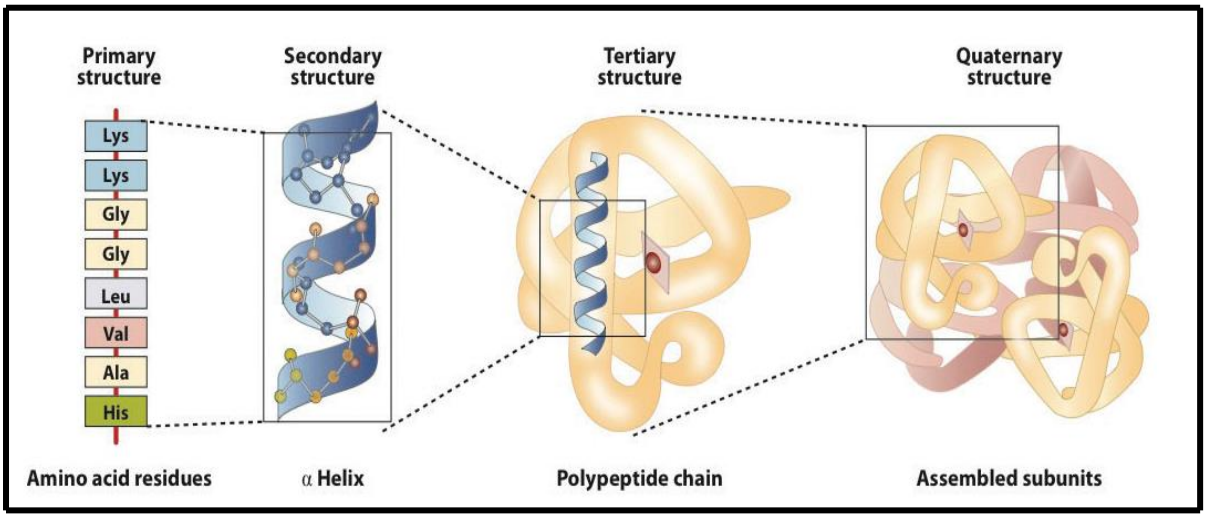

Figure1.6: Level of structures in proteins[14]

Proteins and peptides have wide variety of functions such as enzymes for catalysis, antibodies for molecular recognition, peptide hormones and so on. Among this the cell penetrating peptides (CPP) are of great interest. They are cationic or amphipathic peptides which can cross the cell membrane and enter into the cell.[15,16] Transactivating transcriptional activator (TAT) peptide is one of the CPP derived from HIV which can translocate biomolecules, nanoparticles and drugs through the cell membrane without normal endocytic pathways.[17,18]

1.4 Peptide integrated magnetic nanoparticle

Superparamagnetic nanoparticles are used in wide range of applications including magnetic resonance imaging (MRI),[19] site specific drug delivery,[20] DNA sorting,[21] bio separation,[22] and magnetic hyperthermia[23] for specifically treating tumor. Most of these applications require stable water dispersible, highly monodispersed particles with narrow size distribution. However, due to high surface energy nanoparticles tend to attract each other and get agglomerated. Another difficulty experienced with the magnetic nanoparticle in cancer diagnosis is the lack of ability to target the tumor cells. Also lack of efficient permeability through the cell membrane is one of the challenges in drug delivery. One way to overcome these difficulties is to functionalize the surface of magnetic nanoparticles with biomolecules. Such modifications allow changing the toxicological, physical and chemical properties of the particles. Also attachment of peptides, antibodies, genes, DNAs allows us to make multifunctional particles with both magnetic and biological properties. Peptides are able to arrange the amino acids into secondary structures. This gives them chemical diversity, biocompatibility and ability to target molecular recognition site. Among this, cell penetrating peptides are of great interest because of their cellular intake. TAT peptides are cell penetrating peptides derived from HIV-1 which can penetrate through the cell membrane.[24] By integrating magnetic nanoparticles and peptide gives multifunctional particles in nanoscale which can be used for site specific drug delivery, biosensor, cell imaging, and magnetic hyperthermia. The attachment of a fluorescent molecule FITC at the end of this hybrid nanomaterial will act as a biomarker and can be helpful in efficiently studying the uptake and site specific targeting of these molecules.

CHAPETR II

Synthesis and Characterization Techniques

This chapter describes the various synthetic routes used to prepare the peptides and integrating it with the magnetic nanoparticles. The various experimental tools used to study the structure and properties of peptide and peptide integrated magnetic nanostructures are also discussed in this chapter.

2.1 SYNTHESIS

2.1.1 Peptide Synthesis

To integrate with the magnetic nanoparticles we designed 4 peptides in which one is a cell penetrating peptide (P4). The sequences of structures planned for the present investigation is shown in the Figure 2.1.

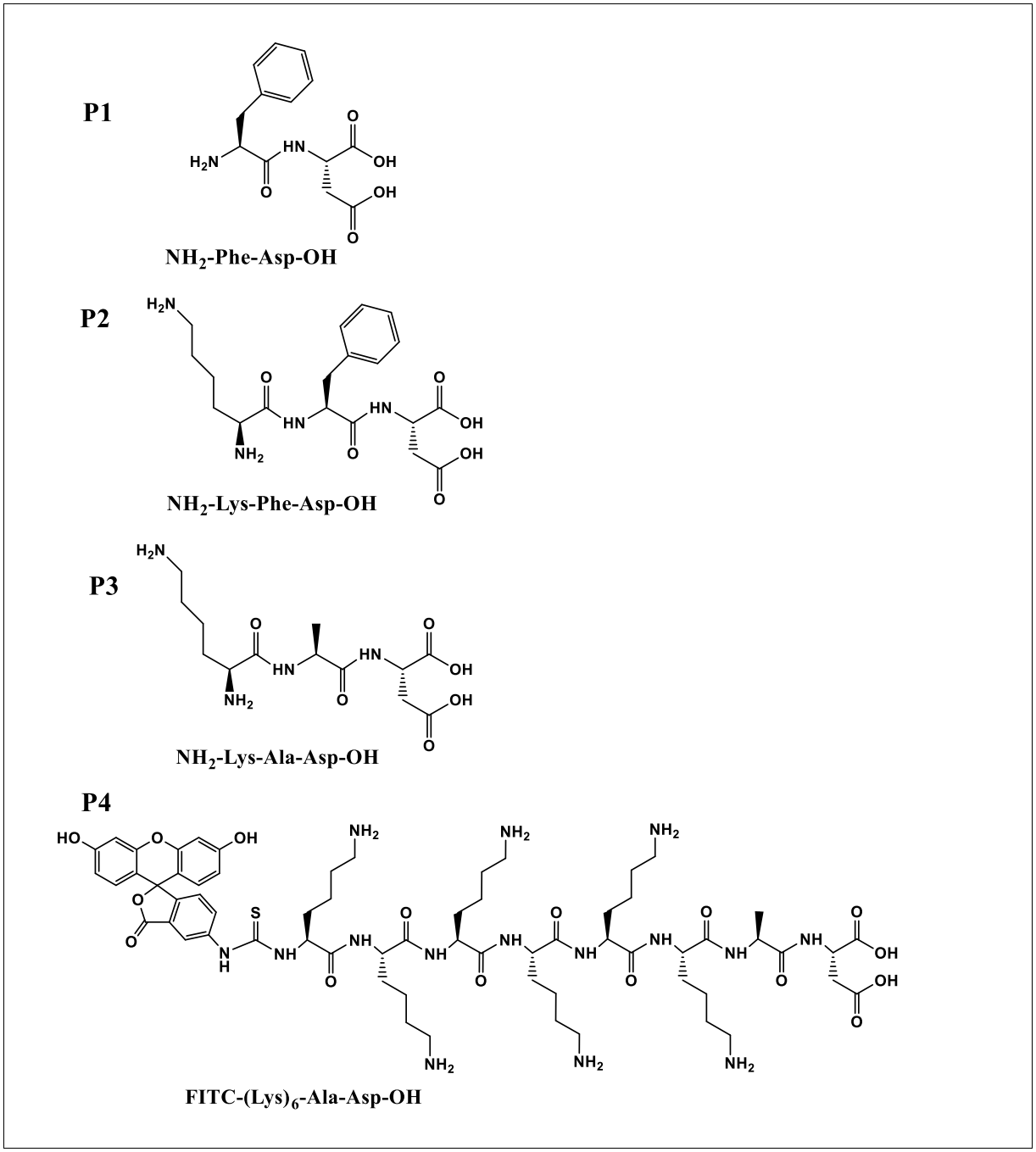

Figure 2.1: Designed peptides

P1, P2 and P3 were synthesized by solution phase peptide synthesis and purification was done by silica column. The cell penetrating peptide P4 was synthesized by solid phase method using HBTU/HOBt as coupling agents on Wang resin. After the synthesis, a fluorescent reagent, FITC was connected at the end. The peptide then was cleaved from resin using pure TFA. The schematic representation of solid phase synthesis of P4 is given in the Figure 2.2.

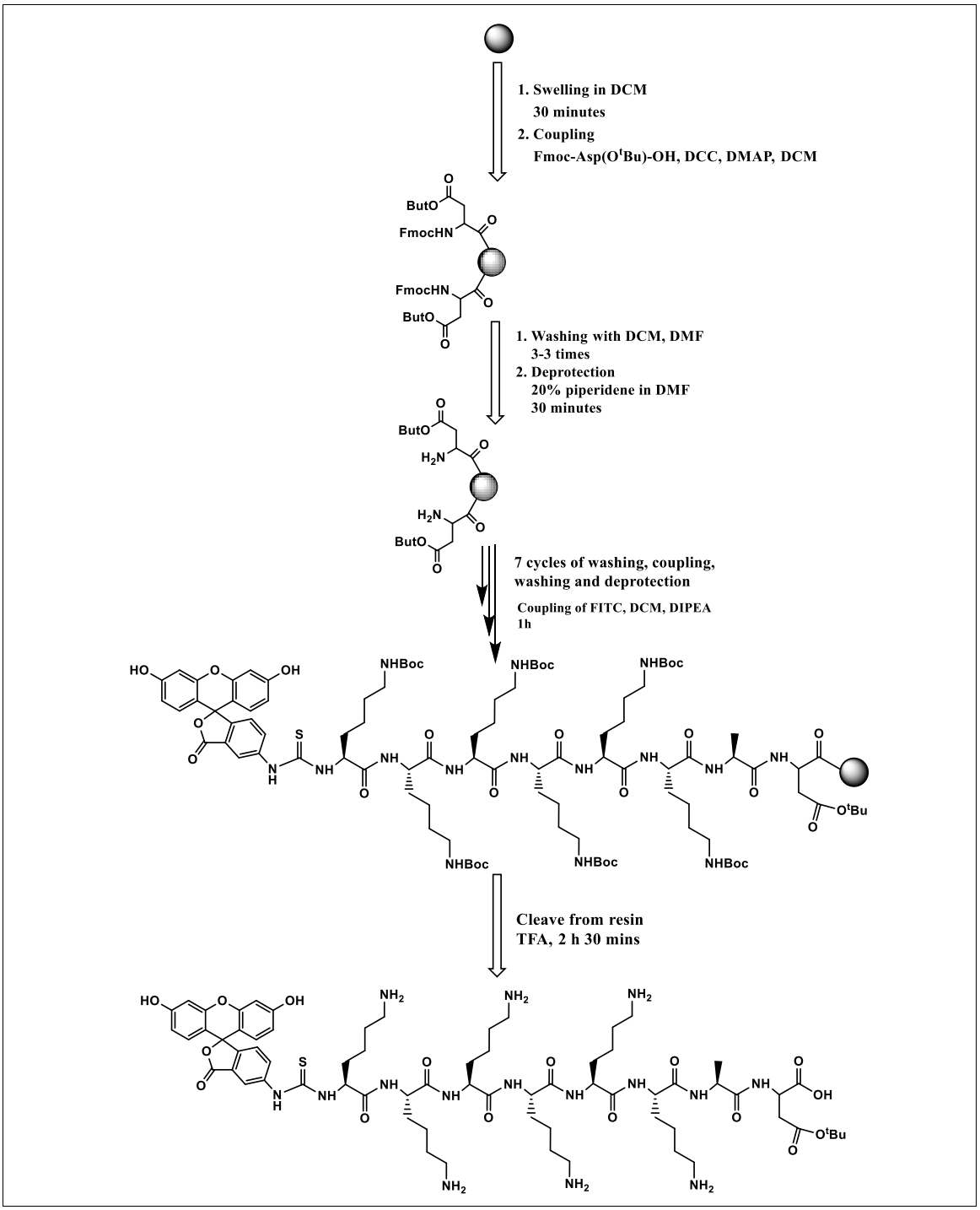

Figure 2.2: Solid phase synthesis of P4

2.1.2 Synthesis of peptide integrated magnetic nanoparticles

Magnetic nanoparticles with peptide were synthesized by high temperature thermal decomposition method[25] using NMP as a solvent and as-prepared peptide as a capping and stabilizing agent. 0.05 M iron acetylacetonate in 10 mL NMP was taken in a pressure equalizer which was attached to a three-neck round-bottom (RB) flask. In a RB flask EDA was mixed with 35ml of NMP and the mixture was magnetically stirred and heated up to 200^{o}C under refluxing condition. When the temperature reached 200^{o}C, iron acetylacetonate solution was injected into RB and was further refluxed for 1 h. Heat source was removed after 1h. When temperature reached ~70 – 80^{o}C the peptide solution was added. After stirring it for nearly 1h at 80^{o} C, the temperature was removed and the mixture was further stirred for ~12 h. The dark brown color product was centrifuged and washed with ethanol and dried in a vacuum oven for further characterization. Cobalt ferrite was also synthesized by using the same method in which $Fe(acac)_3$ and $Co(acac)_2$ were used in the ratio 2:1 respectively. Figure 2.3 shows the schematic diagram of synthesis of peptide integrated magnetic nanoparticles.

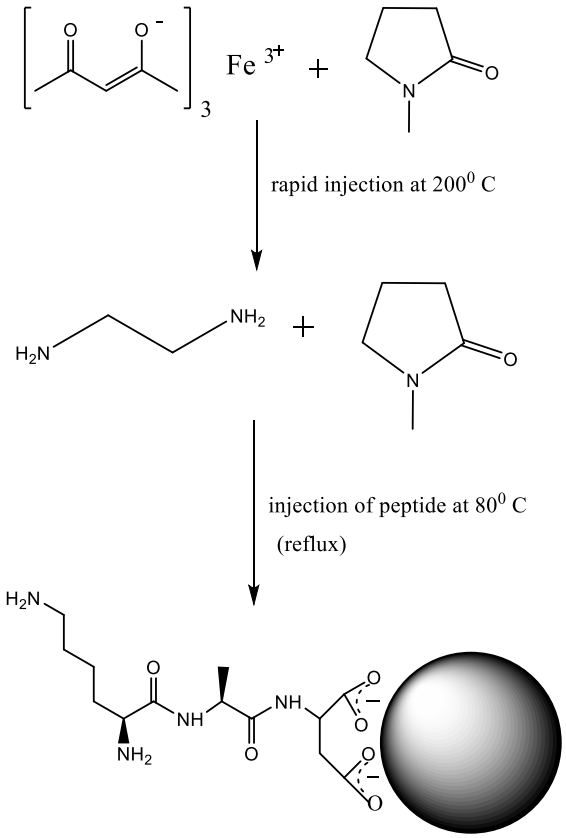

Figure 2.3: Schematic representation of synthesis of MNPs with peptide P3

2.1.3 Synthesis of oleic acid, oleyl amine stabilized iron oxide

Oleic acid, a fatty acid is commonly used for the stabilization of magnetic nanoparticles in organic phase. Similarly oleyl amine also acts as a reducing agent and stabilizer for MNP. We have synthesized MNP using equimolar concentration of both oleic acid and oleyl amine for further studies.[25] The synthesis was carried out by thermal decomposition method as mentioned earlier. Oleic acid and oleyl amine was taken in equal concentration (0.3 M) in 35ml NMP and 1, 2-hexadecanediol (0.3 M) was also added. The mixture was magnetically stirred and heated to reflux at 200^{o}C under the flow of argon. To this $Fe(acac)_3$ was added and further refluxed for 1h. After 1h, heat source was removed and stirred for ~ 12 h. Addition of ethanol gave black precipitate which was washed and centrifuged. Centrifuged product was dissolved in hexane. 100µL of oleic acid and oleyl amine were also added to this and again precipitated by the addition of ethanol. This procedure was repeated for 2-3 times to remove the excess surfactants. The precipitate was dried under vacuum oven for further characterization.

2.1.4 Mesoporous silica coating on oleic acid, oleyl amine coated iron oxide

Coating of iron oxide nanoparticles with mesoporous silica was done by a well-established Stober method.[26] Micro - emulsion was made by taking Fe_2O_3 coated with oleic acid and oleyl amine in chloroform and aqueous solution of CTAB. Heating at 60^{o} C for 10 minutes allowed the evaporation of chloroform. CTAB helps the MNP to come from organic phase to aqueous phase. Ammonia, TEOS and ethyl acetate was further added to the water dispersible particle. The mixture was allowed to stir for 30 seconds and aged for 3h. The precipitate was washed using water and ethanol and dried in vacuum oven.

2.2 MATERIAL CHARACTERISATION TECHNIQUES

2.2.1 X-RAY DIFFRACTION

X-ray powder diffraction is a technique used to identify the phase purity of crystalline materials. It can also be used to identify the crystallite size, lattice parameters, defects, strains and so on. When x-ray is incident on a material, they get diffracted from the atoms of the targeted material. The material with crystalline structure gives characteristic diffraction pattern depending on the arrangements of atoms in the material.[27] The diffraction pattern is different for each material. The diffracted wave intensities depend upon the number of atoms present on the particular diffraction plane.

In a PXRD, the X-rays are generated by a cathode ray tube and directed towards the sample for diffraction to occur. The coming X-ray is incident on the sample at an angle θ and it is diffracted at an angle 2θ. Constructive interference occurs only for certain angles θ where path difference is an integral multiple of wavelength of coming ray. The equation is given by Bragg's law,

$$2d\sin\theta = n\lambda$$

Where, λ is the wavelength of incident ray

d is the inter planar distance

θ is the incident angle

n is an integer called order of diffraction.

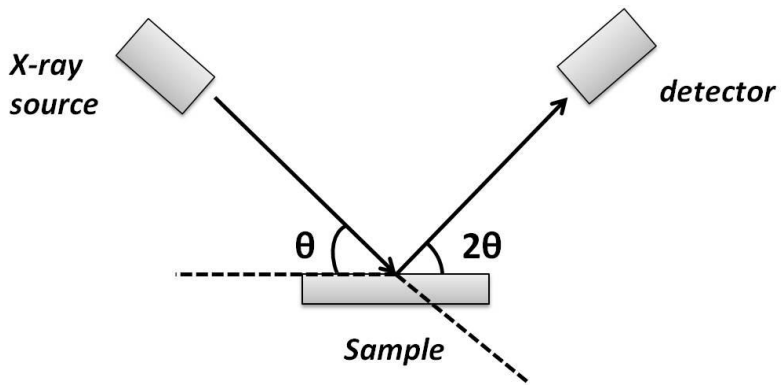

Figure 2.4: Representation of X-ray diffraction

Characterization and phase purity of the samples were done by using a model D8 ADVANCE BRUKER diffractometer at IISER Pune equipped with Ni-filtered CuK_{α} radiation (λ = 1.5417 Å, 40kV and 30mA). The diffraction patterns obtained (I/I_o vs d-spacing) were matched with JCPDS standards. Crystallite size was calculated using Scherrer formula.

2.2.2 Fourier Transform Infrared Spectroscopy

FTIR is a technique used to identify chemical bonds in materials which has a change in permanent dipole moment.[28] It measures the absorption of infrared radiation by the material versus wavelength. The wavelength is measured as wave numbers over the range 4000 – 400 cm^{-1}.

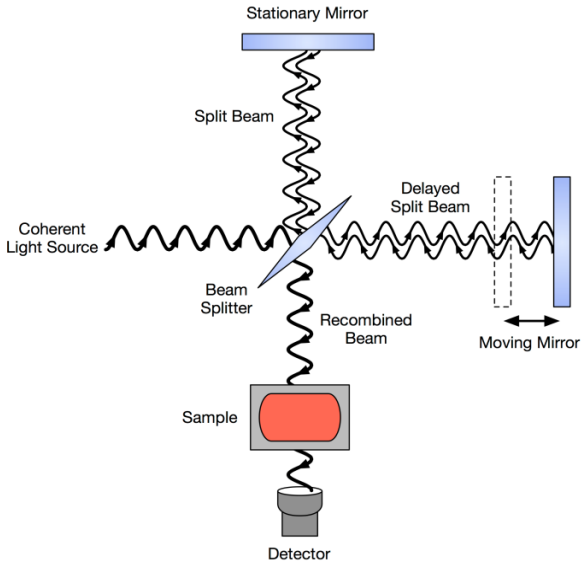

Figure2.5: Schematic representation of FTIR[29]

All the measurements were taken by preparing pellets of IR transparent KBr (Sigma Aldrich, spectroscopy grade) and respective samples and take the measurements for 400 - 4000 cm^{-1} range (Nicolet 6700). The FTIR measurements of these samples were carried out on a Nicolet 6700 FTIR spectrometer at IISER, Pune.

2.2.3 Superconducting Quantum Interference Device (SQUID)

SQUID is a method which allows determining the magnetic moment of materials. Field dependence and temperature dependence of magnetization can be done with this. Temperature variation of magnetization is measured by two methods. In first one sample is cooled in the absence of field from room temperature to a lower temperature. After this, temperature starts increasing and magnetization is measured. This is called zero-field-cooled (ZFC) magnetization. In second method, cooling of sample takes place in the presence of an applied field and then magnetization is measured while warming the sample. This method is called field-cooled (FC) magnetization. The hysteresis loops at 300K and 5K were obtained in a magnetic field varied from +6 to −6 T.

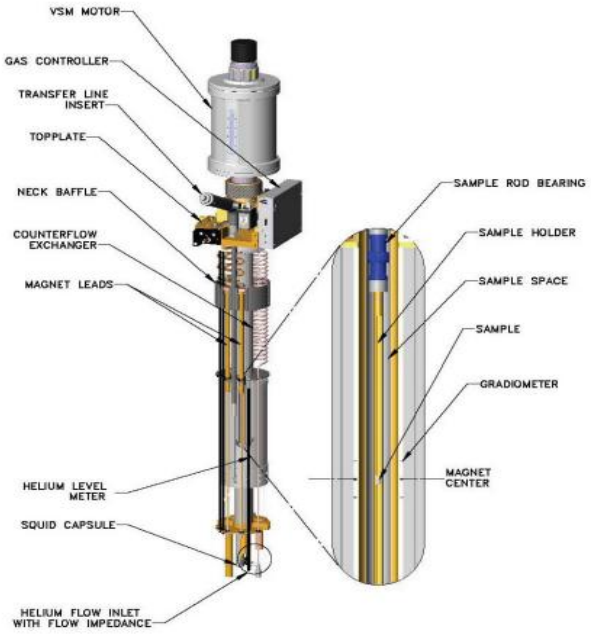

Figure 2.6: Schematic diagram of magnetic property measurement system[30]

2.2.4 Thermogravimetric Analysis

Thermogravimetric analysis (TGA) is a technique which is used to study the weight loss of a material with increasing temperature. In this study, the sample's temperature is varied from room temperature to a high temperature in the

atmosphere of nitrogen, air or in vacuum. TG gives the information about physical phenomena like oxidation, reduction, sublimation, desorption, adsorption, absorption etc.

A Perkin Elmer: STA 6000 thermal analyzer at IISER Pune was used to perform the thermogravimetric analysis. Thermal analysis was carried out up to 1073 K at a heating rate 10^{o}/ min.

2.2.5 UV-Visible Spectroscopy

It is an absorption spectroscopy using electromagnetic waves, wavelength ranging from 200- 800 nm. The UV-Visible light can cause the transition of electrons in a molecule. When light is incident on the surface, the electrons absorbs the light and gives corresponding spectrum. According to Beer-Lambert's law,

$$\text{Absorption, } A = \varepsilon C l$$

Where, ε - molar absorption coefficient of absorbing material

C - concentration

l - path length.

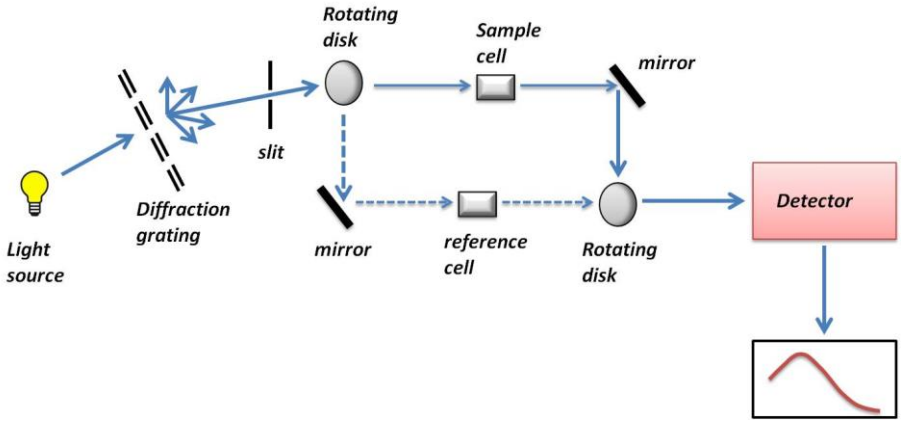

Figure 2.7: Schematic representation of UV-Visible spectrum

All measurements were done by using PERKIN ELMER UV- VIS absorption spectrometer at IISER Pune.

2.2.6 Photoluminescence Spectroscopy

It is a technique used to study electronic properties of material. When light is incident on a material it absorbs energy and get excited. The excess energy is dissipated through emission of light or luminescence. The light can be collected and analyzed to study about the material.

2.2.7 Nuclear Magnetic Resonance Spectroscopy

NMR is a spectroscopic technique used to identify the structure of organic compounds. It exploits the magnetic property of certain atomic nuclei to give the information about structure and chemical environment of molecules.

2.2.8 Matrix Assisted Laser Desorption / Ionization Time of Flight Mass spectroscopy

It is a spectroscopic method to find out the accurate mass of chemical compounds. The compound is mixed with the matrix and ionized using a laser beam. A voltage is applied which moves the charged ions and are detected on the basis of their mass to charge (m/z) ratio.[31]

2.2.9 High Performance Liquid Chromatography

HPLC is a form of column chromatography in which the solvent is pumped through a column under high pressure. It can separate and identify the compounds dissolved in solvents in very low concentrations. The detection is automatic and very sensitive. The measurements were carried out by using Dionex ICS-3000 at IISER Pune.

CHAPETR III

Results and Discussion

This chapter describes an efficient strategy to achieve water dispersible multifunctional $CoFe_2O_4$ and γ-Fe_2O_3 magnetic nanoparticles utilizing NMP as a solvent and tripeptides as a capping agent and a stabilizer. Integration of tripeptides allowed us to further extend the similar protocol to design cell-penetrating fluorescent peptide hybrid magnetic nanostructures suitable for biomedical applications. The multifunctional materials obtained were characterized by XRD, FTIR, TGA, MPMS magnetometer, UV-Vis spectroscopy and Photoluminescence spectroscopy (PL).

3.1 INTRODUCTION

Earlier, we introduced NMP as a strong polar solvent for the synthesis of highly monodispersed magnetic nanoparticles following thermal decomposition method and further, recently, synthesis of nearly monodisperse magnetic nanoparticles by solvothermal route was reported in the literature.[25,32] Both these work provided a simple method for the synthesis of highly monodispersed magnetic nanoparticles dispersible in non-aqueous solvents. NMP being high boiling strong polar solvent, it can be exploited to develop a generic approach for obtaining water dispersible nanoparticles simply by appropriate surface functionalities. In this direction, we utilized peptides of different functionalities as a surfactant and stabilizing agent to make water dispersible multifunctional magnetic nanostructure suitable for biomedical applications. In order to have direct comparison, we also synthesized magnetic nanoparticles without peptides with NMP as a high boiling solvent.

3.2 Synthesis of peptides

The peptides P1, P2 and P3 were synthesized by solution phase synthesis and were characterized by NMR spectra. To start with, we designed a simple dipeptide P1 and then further added one more amino acid with this sequence to prepare P2. The peptides were then used to synthesize water dispersible magnetic nanoparticles by a thermal decomposition method. The nanoparticles prepared with P1 and P2 were water dispersible but settled very fast within few minutes. In order to make the particles stable in water, we designed a tripeptide P3 which was further characterized by NMR spectra (see Figure 3.1).

^{1}H NMR (400MHz, chloroform-d) δ 7.06 (d, *J* = 6.3 Hz, 1H), 6.75 (d, *J* = 7.3 Hz, 1H), 5.23 (s, 1H), 4.83-4.81 (m, 2H), 4.12-4.05 (m, 2H), 3.12-3.10 (m, 2H), 3.01 (dd, *J* = 17.2, 4.8 Hz, 1H), 2.84 (dd, *J* = 17.2, 4.8 Hz, 1H), 1.72 (s, 10H), 1.51-1.36 (m, 28 H)

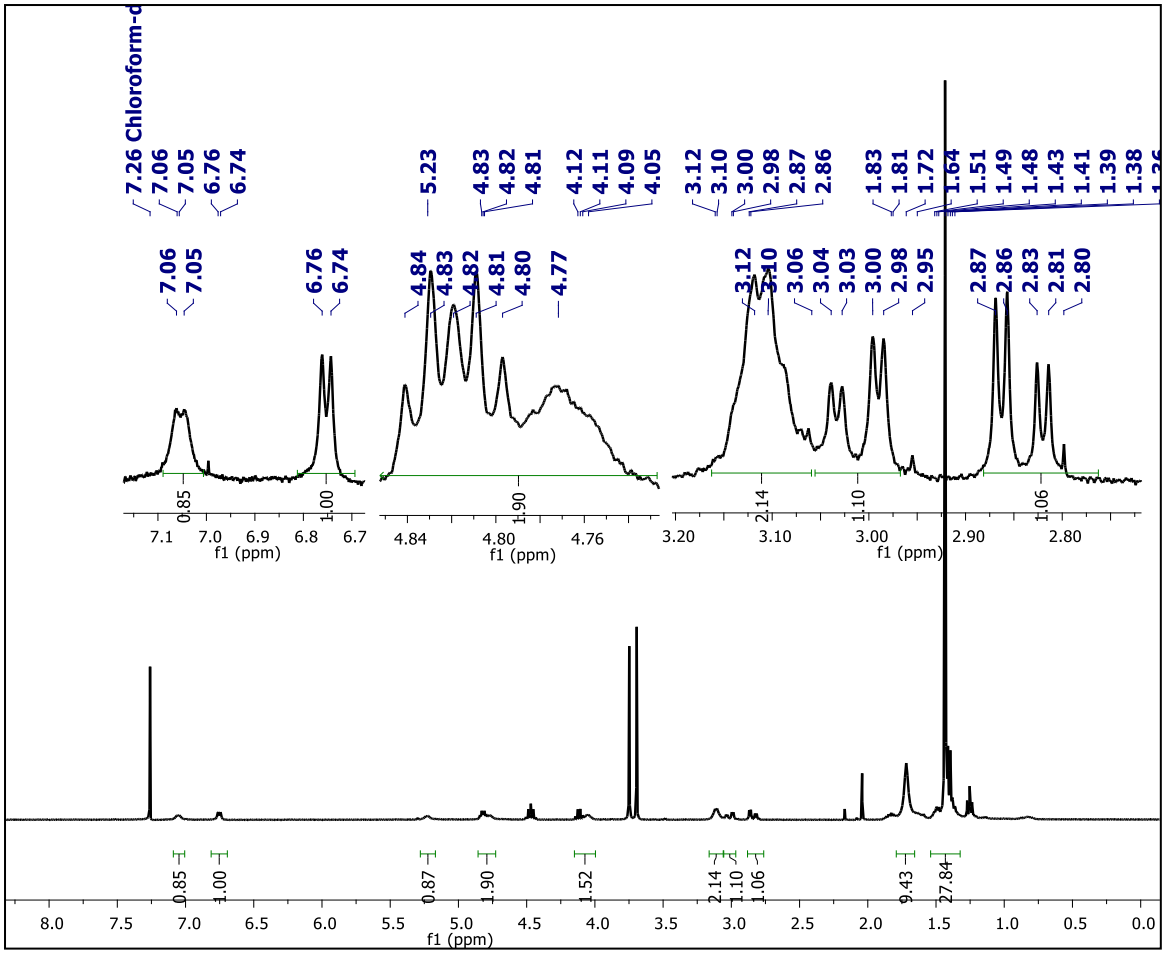

Figure 3.1: NMR spectra of P3

3.3 Peptide integrated magnetic nanoparticles

Using P3 as a capping and stabilizing agent we have synthesized γ-Fe_2O_3 and $CoFe_2O_4$ nanoparticles. Integration of peptide was done by the procedure as mentioned in chapter 2. To understand the mechanism of attachment of peptide and how it changes the properties, we have synthesized MNP without any peptide (Fe-NMP) utilizing NMP as a solvent and keeping all other parameters fixed. These nanoparticles without P3 were further compared with the peptide hybrid magnetic nanoparticles and the results are discussed below.

Figure 3.2 shows the comparison of PXRD patterns of nanoparticles prepared with and without the peptide P3. The peak positions and relative intensity of the reflection matches well with the simulated patterns of bulk $CoFe_2O_4$ (a = 8.3919 Å, JCPDS no. 22-1086) and γ-Fe_2O_3 (a = 8.3967 Å, JCPDS no. 19-629), indicating the formation of pure phase of magnetic nanoparticles. It is interesting to see that the Bragg reflection peaks are all relatively broad with P3 and this may be attributed to the formation of smaller, non-interacting magnetic nanoparticles.

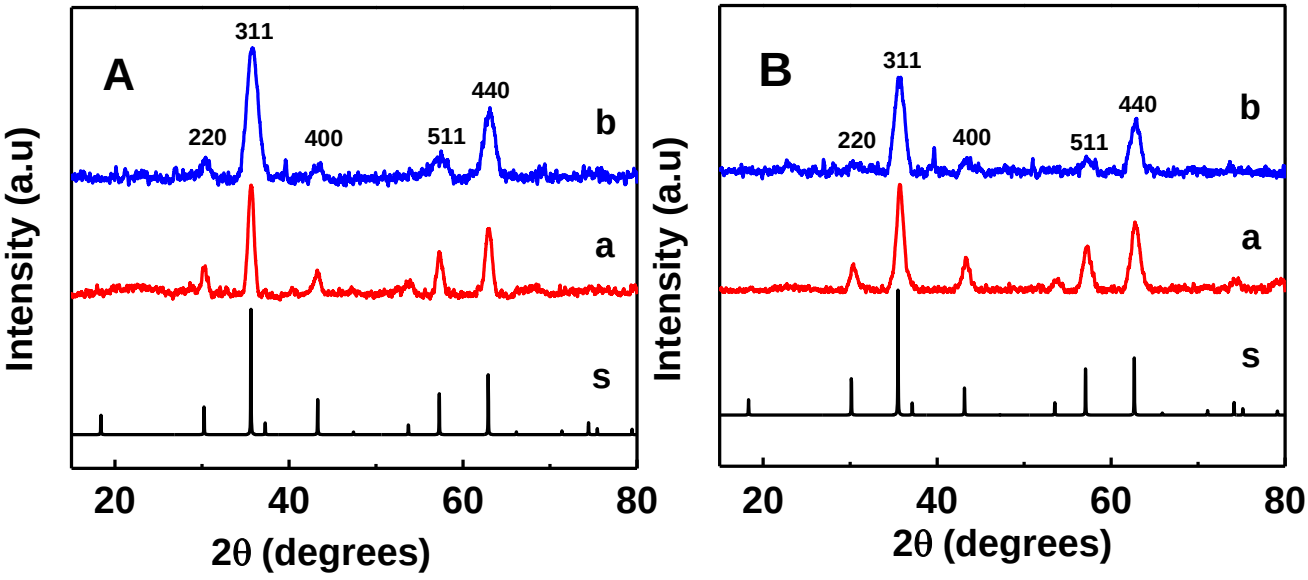

Figure 3.2: PXRD patterns of iron oxide (A) and cobalt ferrite (B) synthetized without P3 (a) and with P3 (b) respectively. S is the simulated patterns of γ-Fe_2O_3 (left) and $CoFe_2O_4$ (right) with a = 8.396 Å and 8.3919 Å respectively.

The average crystallite sizes with the P3 as a surfactant were estimated to be about 6 and 8 nm respectively for $CoFe_2O_4$ and Fe_2O_3 nanoparticles. Interestingly, larger crystallite sizes of ~9 and ~11 nm were observed respectively for $CoFe_2O_4$ and Fe_2O_3 nanoparticles when synthesized without peptides, indicating the formation of bigger particles due to higher surface energy of the particles. The calculated cubic lattice parameters are 8.39 Å and 8.388 Å respectively for the samples $CoFe_2O_4$ and Fe_2O_3 and are comparable to that obtained for the bulk samples.

Figure 3.3 shows the FTIR spectra of γ- Fe_2O_3 and $CoFe_2O_4$ nanoparticles prepared with and without peptide P3. The characteristic spinel absorption bands at ~ 610cm^{-1} confirms the formation of $CoFe_2O_4$ and γ-Fe_2O_3 ferrite phases. Presence of strong NH stretching mode at ~ 3400 cm^{-1} both in the $CoFe_2O_4$ and Fe_2O_3 nanostructure confirms the adsorption of peptides on the surface of the nanoparticles. Presence of C=O stretching mode around 1700 cm^{-1} for the magnetic nanoparticles without peptides clearly reveals that NMP itself acted as a capping agent which may undergo ligand exchange upon treatment with peptides.

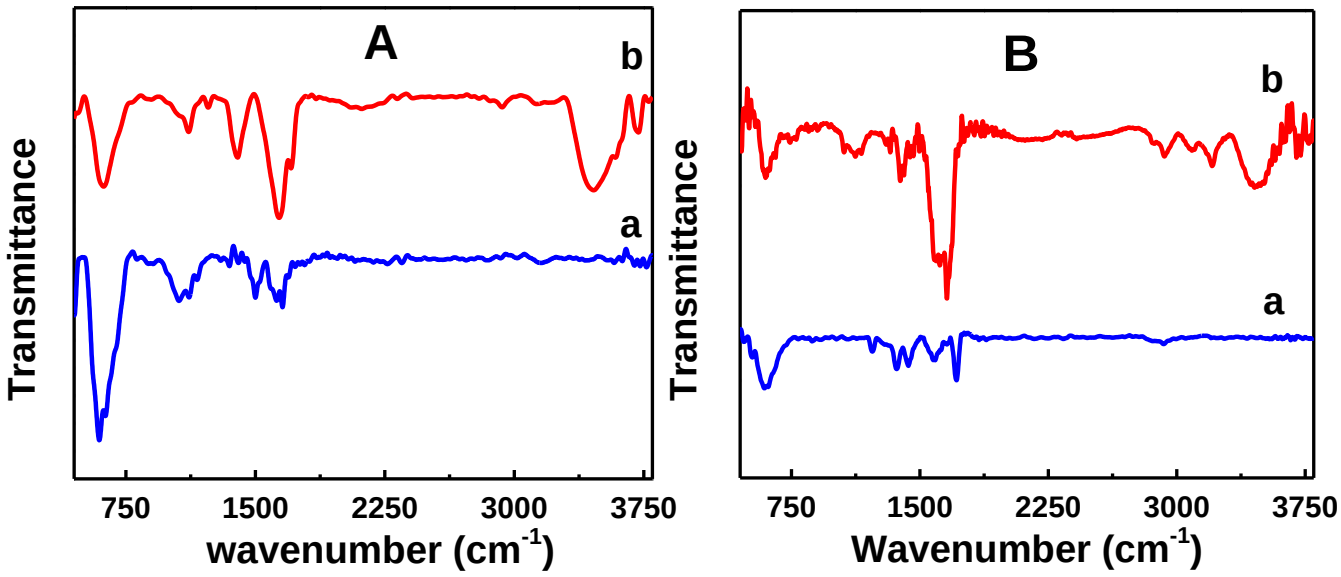

Figure 3.3: FTIR spectra of (A) γ-Fe_2O_3 and (B) $CoFe_2O_4$ without P3 (a) and with P3 (b)

In order to quantify the peptides on the surface of magnetic nanoparticles we performed TGA analysis on MNPs prepared with and without peptide P3. In this experiment the particles were heated from room temperature to 700^oC and the loss of weight due to the decomposition of surfactant was measured. Figures 3.4A and B represent TGA data of the iron oxide and cobalt ferrite nanoparticles with and without peptide P3. From the extra weight loss of ~ 40% in the case of iron oxide and ~75% in the case of cobalt ferrite as compared to the corresponding weight loss of the nanoparticles prepared without peptides clearly reveal the presence of peptide on the surface of the nanoparticles.

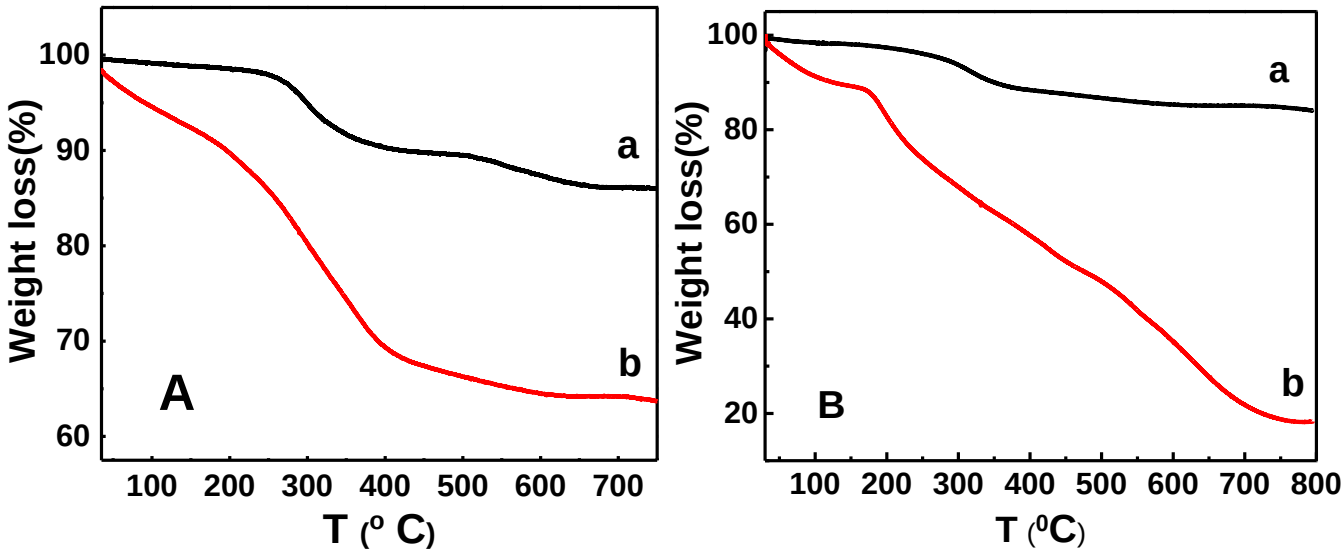

Figure 3.4: TGA of iron oxide (A) and cobalt ferrite (B) without peptide (a) and with peptide respectively

Figure 3.5 illustrates the field dependent magnetic properties of γ-Fe_2O_3 and $CoFe_2O_4$ nanoparticles measured at 300K. It is interesting to note that both for Fe_2O_3 and $CoFe_2O_4$ nanoparticles synthesized with and without peptides, the magnetization does not saturate even for the applied field as strong as 50 Oe and the hysteresis is not present. The M-H curves show the characteristic properties of superparamagnetism for all the magnetic nanoparticles (see insets A, B, C, D Figure 3. 5). The saturation magnetization at room temperature can be estimated by extrapolating 1/H → 0 from the M versus 1/H curves. The room temperature saturation magnetization values obtained were 60.5 emu/g and 65.8 emu/g respectively for $CoFe_2O_4$ and Fe_2O_3 nanoparticles without any peptides on the surface. It is interesting to note that the saturation magnetization of these nanoparticles is less than the bulk values (80-85 emu/g) of $CoFe_2O_4$ and γ-Fe_2O_3 nanoparticles. The saturation magnetization values for both $CoFe_2O_4$ and γ-Fe_2O_3 nanoparticles showed a substantial decrease to the value of 15 emu/g and 12 emu/g respectively on the coating with the peptide. A large decrease in the saturation magnetization value is attributed to both reduced particle sizes as evident from XRD crystallite size calculations and also the broken exchange interactions predominantly on the surface of each particle. This in turn led to the existence of non-collinear frustrated spins on the surface of the particles.

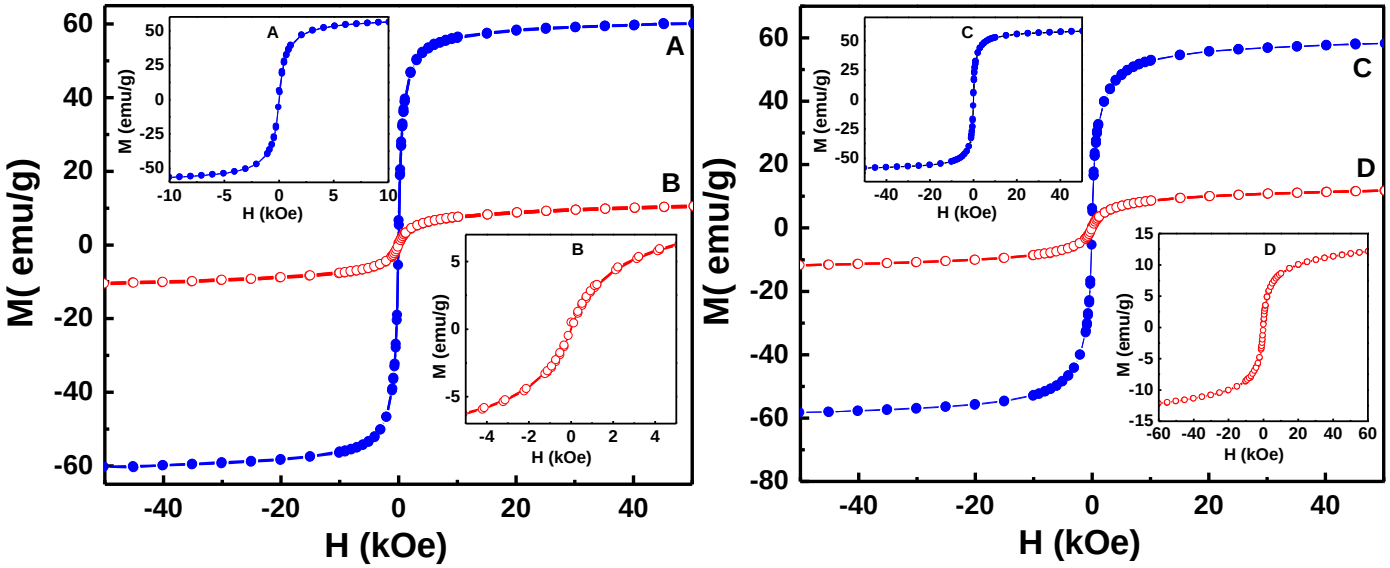

Figure 3.5: Field dependent magnetization at 300 K for γ-Fe_2O_3 (left) and $CoFe_2O_4$ (right) nanoparticles synthesized without P3 (A, C) and with P3 (B, D). Insets represent corresponding expanded magnetization at low field.

Figure 3.6 represents temperature dependent magnetization behavior of the magnetic nanoparticles measured at 50 Oe. Superparamagnetic particles are characterized by zero-field-cooled (ZFC) and field-cooled (FC) magnetization. In ZFC measurements, first the sample was cooled from room temperature to 5 K in the absence of an applied field, and then the magnetization was measured while warming after applying a field of 50 Oe. For field-cooled (FC) measurements, the samples were cooled from room temperature to 5 K in the presence of a field of 50 Oe and magnetization was measured while warming the sample in the presence of the same field. A comparison of the nature of ZFC and FC magnetization curves of Fe_2O_3 and $CoFe_2O_4$ nanoparticles with and without peptides clearly indicated that peptides favored the formation of monodisperse particles with minimum inter-particle interactions. However, in the absence of peptide, there is a strong inter-particle interaction. This is clearly evident from the nature of FC curve (nearly constant magnetization value) below blocking temperature.[25] A shift in the blocking temperatures from ~ 140 K to 84 K and 260 K to 170 K for γ-Fe_2O_3 and $CoFe_2O_4$ nanoparticles respectively indicated change in the anisotropy energy with

the coating of the nanoparticles. Moreover, the bifurcation in ZFC and FC curves and the broadening in the ZFC peak clearly indicate wider particle size distribution with larger fractions of bigger particles in the samples prepared without peptides.

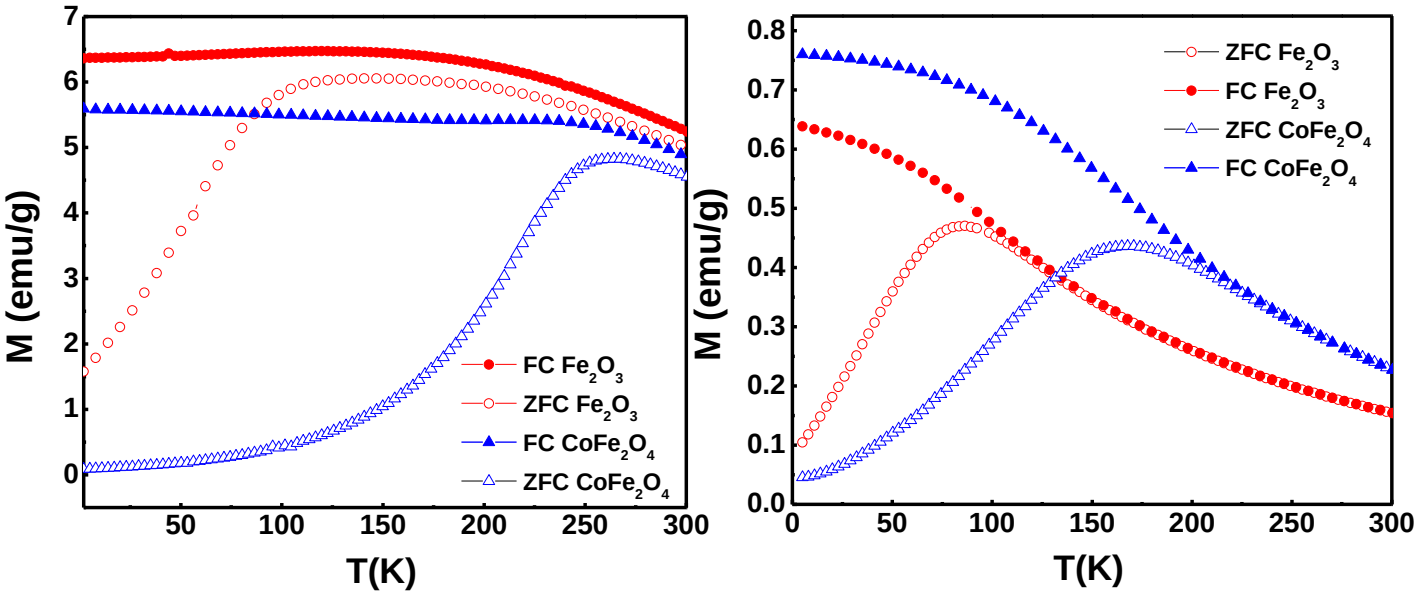

Figure 3.6: ZFC and FC magnetization curves, measured at 50 Oe for magnetic nanoparticles synthesized without peptide (left) and with peptide (right).

The opening of the hysteresis loop below the blocking temperatures is represented in the Figure 3.7. The higher value for T_B in $CoFe_2O_4$ nanoparticles also indicate the higher value of anisotropy and are evident from the higher coercivity for $CoFe_2O_4$ nanoparticles than that of the Fe_2O_3 nanoparticles. Asymmetric hysteresis loop for the particles obtained without peptides indicated partial oxidation of the surface of nanoparticles which may lead to the presence of mixed magnetic phases. Interestingly, with peptide as surfactant, the coercivity of the nanoparticles is higher and the nature of the symmetric hysteresis loop is evident for the absence of the secondary or any mixed magnetic phase.

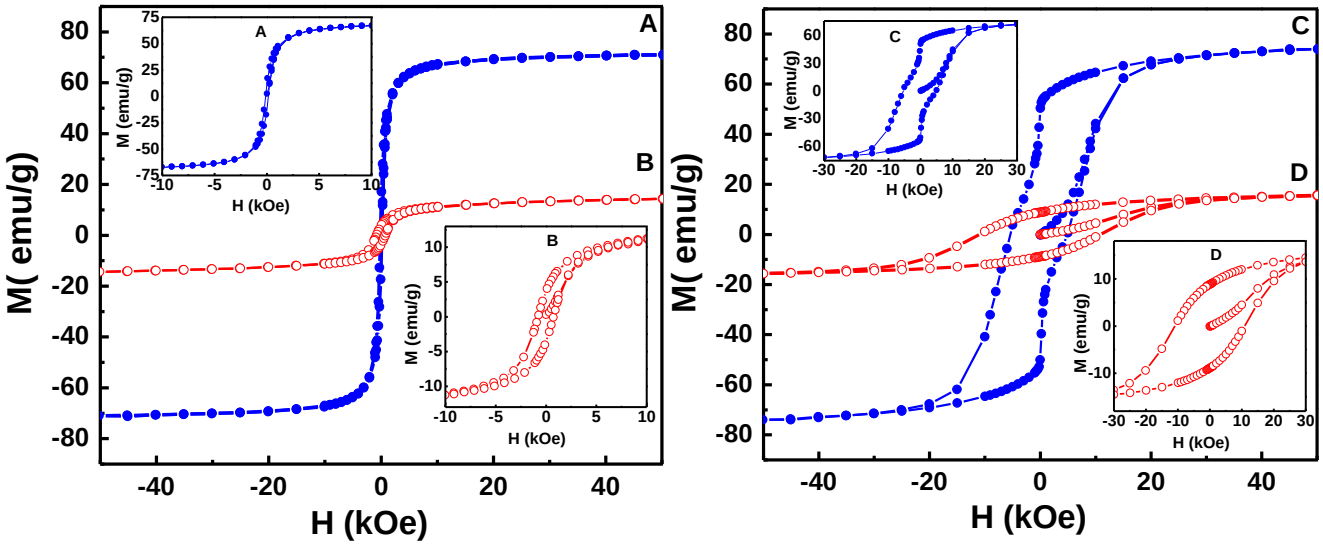

Figure 3.7: Field dependent magnetization at 5 K for γ- Fe_2O_3 (left) and $CoFe_2O_4$ (right) nanoparticles synthesized without peptide (A, C) and with peptide (B, D). Insets represent corresponding expanded magnetization at low field.

Water dispersiblity and the response of magnetic nanoparticles with and without peptide towards a magnet are shown in Figure 3.8.

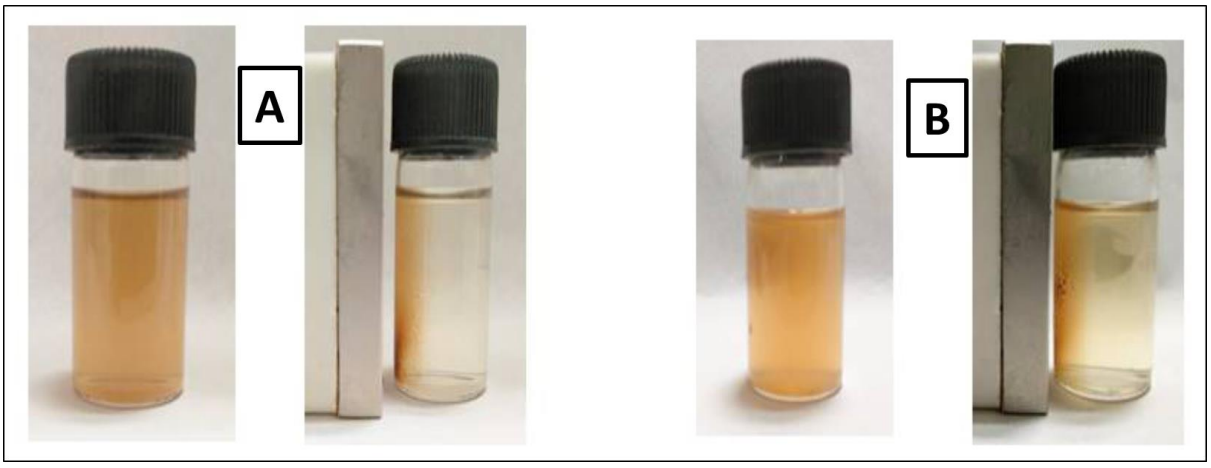

Figure 3.8: Water dispersibility of peptide hybrid (A) γ-Fe_2O_3 and (B) $CoFe_2O_4$ magnetic nanoparticles before (left) and after (right) magnetic enrichment with the external magnet.

From the above PXRD, FTIR, TGA and magnetic measurement data analysis, we concluded the presence of NMP on the surface of the magnetic nanoparticles. However, the particles were found to settle down within few minutes indicating that nanoparticles were not well protected with NMP and hence they tend to get agglomerated due to high surface energy. Based on the initial experimental evidences, the schematic representation of the nanoparticles synthesis without P3 is shown in the Figure 3.9.

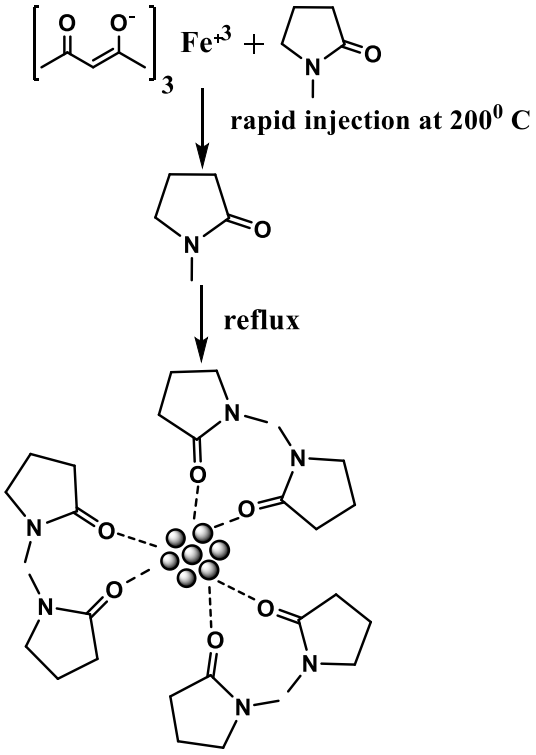

Figure 3.9: Schematic representation of attachment of NMP on the surface of magnetic nanoparticles

The superparamagnetic properties exhibited by MNP with P3 are suitable for biological applications. To exploit this superparamagnetic property of magnetic nanoparticles in biological field, we have designed a cell penetrating peptide P4 which can translocate through the cell membrane. The integration of these two will help in making multifunctional nanoparticles. Cell penetrating peptides can go through the cell membranes which facilitates the cellular uptake of biological molecules and nanostructured material for research work and as medicines. The peptide P4 was synthesized by solid phase method. To investigate the uptake of cell penetrating peptide attached to MNP, a fluorescent dye FITC was attached at the N

terminal of peptide. FITC acts as a bio-marker and the cellular uptake of CPP can be studied by fluorescence microscopy.

A schematic for the attachment of FITC with cell penetrating peptide is shown in the Figure 3.10.

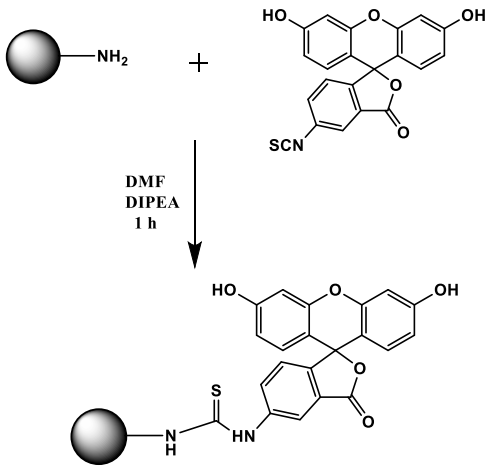

Figure 3.10: Schematic representation of attachment of FITC with CPP

FITC was directly added to the synthesizer after the deprotection of Fmoc from the N terminal of CPP. Reaction was kept for nearly 1h under N_2 flow. Excess monomers were removed by washing it with DCM and DMF. Purification was done by using HPLC. Figure 3.11 shows the HPLC trace of purified P4. The high intense peak at 17 minutes corresponds to P4.

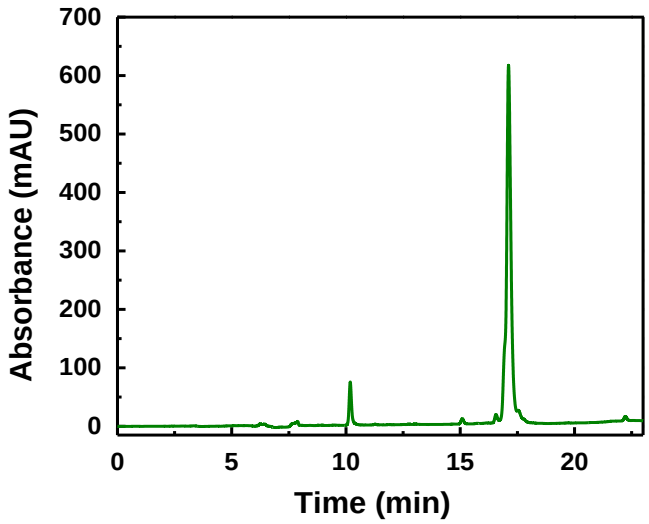

Figure3.11: HPLC trace of P4

Further characterization of P4 was done by using MALDI/TOF. Figure 3.12 shows the MALDI spectra of P4. Expected mass was, [P4 + H^+] = 1363. Well characterized P4 was then used to prepare MNPs as discussed earlier with P3.

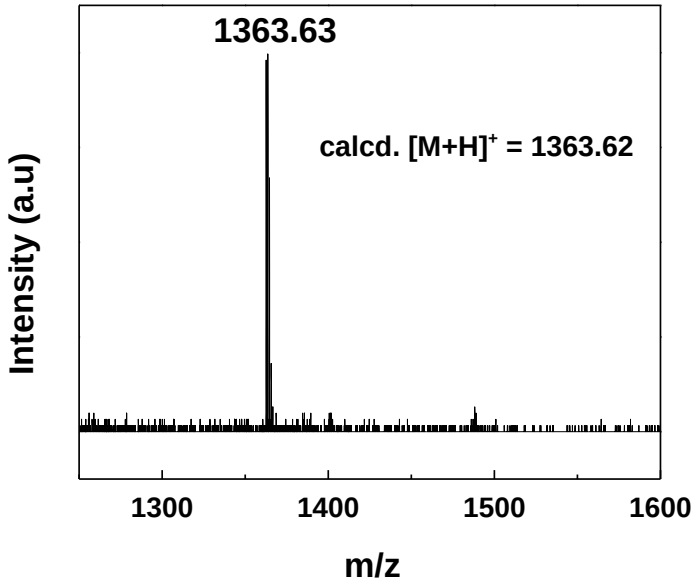

Figure 3.12: MALDI spectra of cell penetrating peptide with FITC

Fluorescent property of MNP-P4 was further studied by UV-Visible spectroscopy. Figure 3.13 compares the UV-VIS spectra of FITC, nanoparticles attached to CPP-FITC and CPP only. The fluorescent dye FITC shows the characteristic peak at 490 nm. The characteristic peak around 490 nm for magnetic nanoparticles attached with CPP-FITC indicate fluorescent behavior of the hybrid structure. In order to prove that the characteristic absorption in UV-VIS spectra is coming from CPP-FITC attached to magnetic nanoparticles only and not from the physical mixture, we took UV-VIS absorption studies of the supernatant after magnetic separation. Absence of any UV-VIS absorption from the supernatant (see Figure 3.13 insets g and f) confirms the attachment of CPP-FITC to the surface of the magnetic nanoparticles. However much work in this direction is required to avoid the expected quenching of fluorescence due to the presence of magnetic nanoparticles.

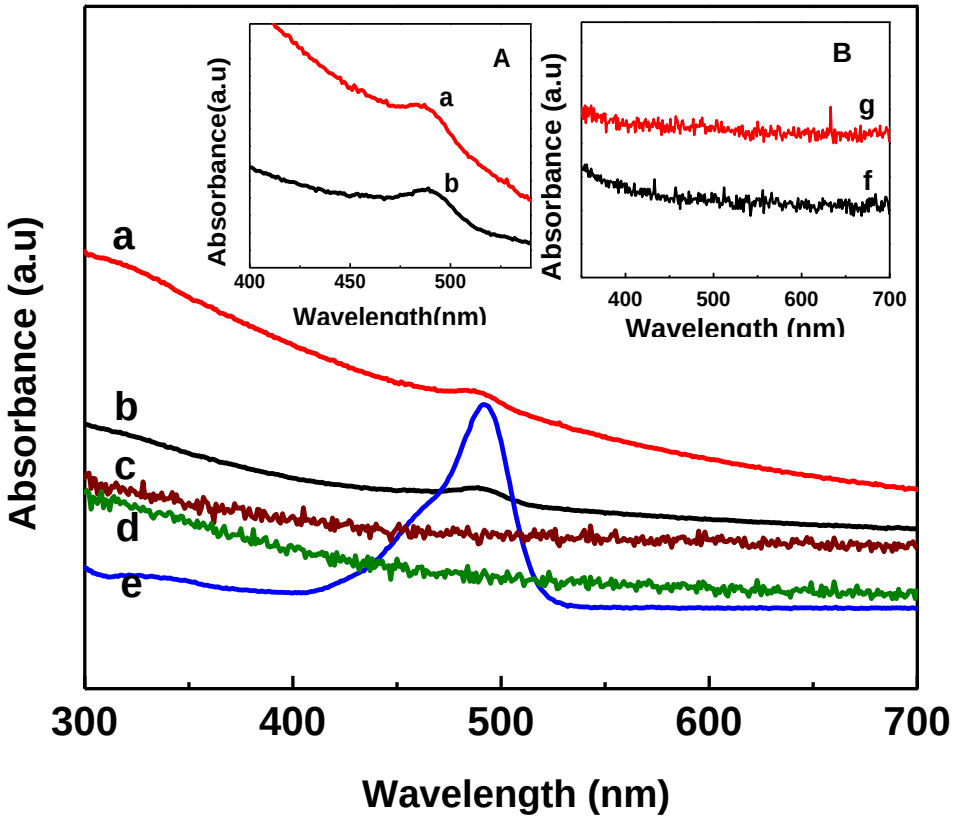

Figure 3.13: UV-Visible spectra of (a) CoFe-P4 (b) Fe-P4 (c) CoFe-CPP (d) Fe-CPP (e) FITC. Absorbance of CoFe-CPP and Fe-CPP are shown in insets (A). Inset (B) supernatant of (g) Fe-P4 and (f) CoFe-P4

In order to study the fluorescent properties of MNPs formed with P4, photoluminescence study was performed. Figure 3.14 illustrates the fluorescence emission spectra (PL) of magnetic nanoparticles functionalized with CPP-FITC. Presence of fluorescence maxima at 524 nm from the excitation wavelength at 488 nm clearly indicated the attachment of FITC-CPP with MNPs.

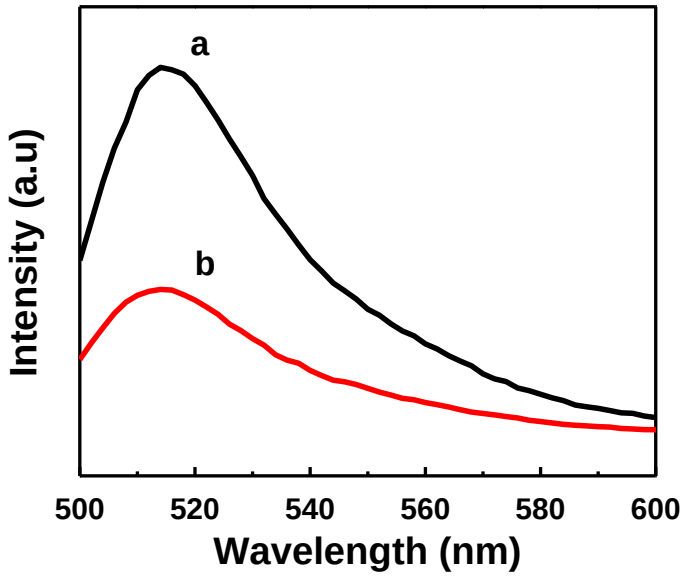

Figure 3.14: Photoluminescence (PL) spectra of attached FITC-CPP with (a) iron oxide (b) Cobalt ferrite

3.4 Challenges

It is expected that nanoparticle's fluorescence gets largely quenched in the presence of magnetic nanoparticles..[34] Iron has emission suppressing effect which results in strong quenching of fluorescence. Cations with partially filled d orbitals can involve in the electron transfer and energy transfer from/ to the fluorophore which quenches its intensity partially or completely.[35] In order to overcome this difficulty, we first coated the MNPs with biodegradable silica shell before attaching that with CPP-FITC. This will not only help us in achieving water dispersible fluorescent magnetic nanostructures but also provide a platform for obtaining biocompatible reactive surface for further bio conjugation. Work in this direction is in progress.

3.5 Synthesis of mesoporous silica on oleic acid, oleyl amine stabilized magnetic nanoparticles

Oleic acid and oleyl amine coated samples were synthesized by already reported thermal decomposition method.[25] The well characterized samples were further phase transferred using CTAB and coating of silica was done by a modified Stober method to obtain a uniform spherical coating.

Morphology of the particles was investigated by FESEM (see Figure 3.15) which clearly indicated the formation of ~100 nm spherical particles. The core-shell morphology of the particles with controllable thickness of SiO_2 needs to be confirmed with TEM analysis and the work in this direction is in progress.

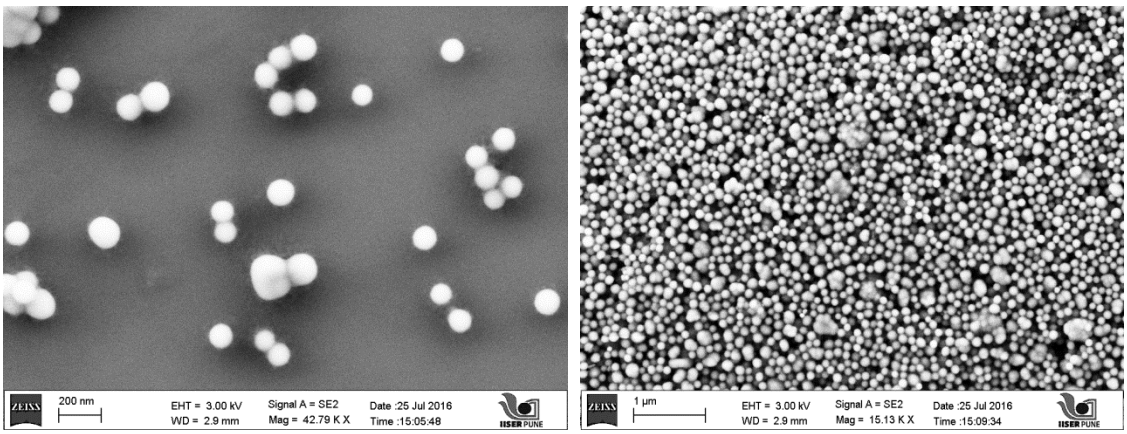

Figure 3.15: FESEM image of silica coated iron oxide

Conclusion

In the present investigation, efforts were made to synthesize water dispersible, highly monodispersed biologically active magnetic nanoparticles by integrating it with cell-penetrating peptide. A one-pot thermal decomposition method utilizing NMP as a high boiling solvent were used for the synthesis of nanoparticles whereas peptides acted both like surfactant as well as stabilizing agent. Average crystallite sizes calculated from PXRD of particles synthesized with peptides were around 6 and 8 nm respectively for $CoFe_2O_4$ and γ-Fe_2O_3 which were much less than the particles synthesized without peptides. Field dependent magnetization curves confirmed the superparamagnetic behaviour of these particles which were suitable for biological applications. Incorporation of cell-penetrating peptides as a surfactant and a stabilizing agent may offer a novel platform to obtain good quality water dispersible biocompatible nanoparticles suitable for biomedical applications.

Future prospects

The biological applications of magnetic nanoparticles synthesized with fluorescent cell penetrating peptide such as site specific drug delivery and magnetic resonance imaging needs to be explored. Also to prevent the quenching of fluorescence the magnetic nanoparticles is being coated with inorganic materials such as SiO_2 and the work in this direction is in progress.

References

1. Shubayev, V. I.; Pisanic, T. R.; Jin, S. Magnetic nanoparticles for theragnostics. *Advanced Drug Delivery Reviews*. **2009,** 61, 467–477.
2. Jun, Y.; Lee, J.; Cheon, J. Chemical Design of Nanoparticle Probes for High Performance Magnetic Resonance Imaging. *Angew. Chem. Int. Ed.* **2008**, 47, 5122 – 5135.
3. Sulek, S.; Mammadov, B.; Mahcicek, D. I.; Sozeri, H.; Atalar, R.; Tekinay, A. B.; Guler, M. O. Peptide functionalized superparamagnetic iron oxide nanoparticles as MRI contrast agents. J*. Mater. Chem.,* **2011**, 21, 15157–15162.
4. Deng, M.; Huang, Z.; Zou, Y.; Yin, G.; Liu, J.; Gu, J. Fabrication and neuron cytocompatibility of iron oxide nanoparticles coated with silk-fibroin peptides. *Colloids and Surfaces B: Biointerfaces*. **2014**, 116, 465–471.
5. Chertok, B.; Moffat, B. A.; David, a. E.; yu, F.; Bergemann, C.; Ross, B. D.; Yang, V. C. Iron Oxide Nanoparticles as a Drug Delivery Vehicle for MRI Monitored Magnetic Targeting of Brain Tumors. *Biomaterials*. **2008**, 29, 487–496.
6. Nitin, N.; LaConte, L. E. W.; Zurkiya, O.; Hu, X.; Bao, G. Functionalization and peptide-based delivery of magnetic nanoparticles as an intracellular MRI contrast agent. *J Biol Inorg Chem*. **2004**, 9, 706–712.
7. Ravindranath, S. P.; Mauer, L. J.; Deb-Roy, J.; Irudayaraj, J. Biofunctionalized Magnetic Nanoparticle Integrated Mid-Infrared Pathogen Sensor for Food Matrixes. *Anal. Chem.*, **2009**, *81*, 2840–2846.
8. Keivit, F. M.; Zhang, M. Surface Engineering of Iron Oxide Nanoparticles for Targeted Cancer Therapy. *Acc. Chem. Res.*, **2011**, *44*, 853–862.
9. F. Yang, D.L. Fu, J. Long, Q.X. Ni, Magnetic lymphatic targeting drug delivery system using carbon nanotubes, *Med. Hypotheses*,**2008**, 70, 765–767.
10. B. D. Cullity, Introduction to Magnetic Materials, Addisson Wesely, Reading MA, 1972.
11. Coll, A. P.; Farooqui, I. S.; O'Rahilly, S. The Hormonal Control of Food Intake. *Cell*, **2007**, 129, 251-262.
12. Tian, L.; Heyduk, T. Antigen Peptide-Based Immunosensors for Rapid Detection of Antibodies and Antigens. *Anal. Chem.*, **2009**, 81, 5218–5225.

13. Rad-Malekshahi, M.; Lempsink, L.; Amidi, M.; Hennink, W. E.; Mastrobattista, E. Biomedical Applications of Self-Assembling Peptides. *Bioconjugate Chem.,* **2016**, 27, 3−18
14. The structure levels in proteins http://xray.bmc.uu.se/kurs/BSBX2/practicals/practical_2/practical_2.html
15. Schmidt, N.; Mishra, A.; Lai, G. H.; wong, G. C. L. Arginine rich cell penetrating peptides. *FEBS Letters*, **2010**, 584, 1806-1813.
16. Morris, M. C.; Deshayes, S.; Heitz, F.; Divita, G. Cell-penetrating peptides: from molecular mechanisms to therapeutics. *Biol. Cell*, **2008**, 100, 201-217.
17. Wunderbaldinger, P.; Josephson, L.; Weissleder, R. Tat Peptide Directs Enhanced Clearance and Hepatic Permeability of Magnetic Nanoparticles. *Bioconjugate Chem.*, **2002**, 13, 264−268.
18. Phan, M. D.; Kim, H.; Lee, S.; Yu, C.; Moon, B.; Shin, K.; HIV Peptide-Mediated Binding Behaviors of Nanoparticles on a Lipid Membrane. *Langmuir*, **2017**, 33, 2590−2595.
19. Fu, A.; Wilson, J.; Smith, R.; Mullenix, J.; Earhart, C.; Akin, D.; Guccione, S.; Wang, X.; Gambhir, S. Flourescent Magnetic Nanoparticles for Magnetically Enhanced Cancer Imaging and Targeting in Living Subjects. *ACS Nano,* **2012**, 6, 6862-6869.
20. Veiseh, O.; Gunn, J. W.; Zhang, M. Design and fabrication of magnetic nanoparticles for drug delivery and imaging. *Adv Drug Deliv Rev.*, **2010**, 62, 284-304.
21. Dressman, D.; Yan, H.; Traverso, G.; Kinzler, K W.; Vogelstein, B. Transforming single DNA molecules into fluorescent magnetic nanoparticles for detection and enumeration of genetic variations. *PNAS.* **2003**, 100, 8817-8822
22. Gu, H.; Xu, K.; Xu, C.; Xu, B. Gum arabic modified Fe_3O_4 nanoparticles cross linked with collagen for isolation of bacteria. *Journal of Nanobiotechnology,* **2010**, 8.
23. A. Ito, Y. Kuga, H. Honda, H. Kikkawa, A. Horiuchi, Y. Watanabe, T. Kobayashi, Magnetite nanoparticle-loaded anti-HER2 immunoliposomes for combination of antibody therapy with hyperthermia, *Cancer Lett.* **2004**, 212, 167–175.

24. Zhao, M.; Kircher, M. F.; Josephson, L.; Weissleder, R. Differential conjugation of Tat Peptide to Superparamagnetic Nanoparticles and Its Effect on Cellular Uptake. *Bioconjugate Chem.,* **2002**, 13, 840−844.
25. Verma, S.; Pravarthana, D. One-Pot Synthesis of Highly Monodispersed Ferrite Nanoparticles: Surface Characterization and Magnetic Properties. *Langmuir,* **2011**, 27, 13189-13197.
26. Kim, J.; Lee, J.; Lee, J, E.; Yu, J, H.; Kim, B, C.; An, K.; Hwong, Y.; Shin, C.; Park, J.; Kim, J.; Hyeon, T. Magnetic Fluorescent Delivery Vehicle Using Uniform Mesoporous Silica Spheres Embedded with Monodisperse Magnetic and Semiconductor Nanoparticles. *J. AM. CHEM. SOC*. **2006**,128, 688-689.
27. *Elements of X-ray Diffraction*, ed. by B. D. Cullity,Addison Wesley Publishing, **1978**.
28. *Fundamentals of Molecular Spectroscopy* by Colin N Banwell and Elaine M McCash, 4th Ed., Tata McGraw-Hill Publishing Co. Ltd., **2002**.
29. https://en.wikipedia.org/wiki/Fourier_transform_infrared_spectroscopy
30. http://physique.umontreal.ca/~andrea_bianchi/uploads/Site/SQUID_VSM_User_Manual.pdf
31. Singhal, N.; Kumar, M.; Kanaujia, P K.; Virdi, J S. MALDI-TOF mass spectrometry: an emerging technology for microbial identification and diagnosis. *Front. Microbiol.*, **2015** , 6
32. Thampi, A.; Babu, K.; Verma, S. Large scale solvothermal synthesis and a strategy to obtain Langmuir-Blodgett film of $CoFe_2O_4$ nanoparticles. *Journal of Alloys and Compounds*, **2013**, 564, 143-150.
33. Veeranarayanan, S.; Poulose, A, C.; Mohammed, M, S.; Nagaoka, Y.; Kashiwada, S.; Maekawa, T.; Kumar, D, S. *J.Mater.Chem.B.* **2015**
34. Tan, S, S.; Kim, S, J.; Kool, E, T. Differentiating between Flourescence Quenching Metal Ions with Polyflourophore Sensors Built on a DNA Backbone. *J. Am. Chem. Soc*. **2011**, 133, 2664–2671.
35. Fabbrizzi, L.; Licchelli, M.; Pallavicini, P.; Sacchi, D.; Tanglietti, A. sensing of transition metals through fluorescence quenching or enhancement. *Analyst*, **1996**, 121, 1763- 1768.